Gastroenterology 2025;■:1–15

Targeting Mutual Dependence of Phosphatidylinositol-3-Kinase α/δ and Small Ubiquitin-Like Modifier Signaling in Pancreatic Cancer

Hazal Köse,[1,2] Christian Schneeweis,[3] Philipp Putze,[3] Constanza Tapia Contreras,[4] Laura Ferreiro,[1,2] Leonie Witte,[4] Ilaria Deidda,[4] Frederik Herzberg,[1,2] Sophie Ebert,[4] Juraj Jakubik,[5,6] Leoni Moldaner,[5,6] Jovan Todorovic,[7] Isabelle Träger,[1,2] Chuanbing Zang,[1,2] Uta M. Demel,[1,2] Elisabeth Hessmann,[8,9,10] Marieluise Kirchner,[11,12] Simone Rhein,[13] Jens Hoffmann,[13] Zuzana Tatarova,[5,6,14] Michael Ghadimi,[4] Dieter Saur,[3,15] Kai Kappert,[16] Philipp Mertins,[11,12] **Günter Schneider,**[3,4,9,10,§] **Ulrich Keller,**[1,2,17,§] and **Matthias Wirth**[1,2,4,18,§]

[1]Department of Hematology, Oncology and Cancer Immunology, Charité - Universitätsmedizin Berlin, corporate member of Freie Universität Berlin and Humboldt-Universität zu Berlin, Berlin, Germany; [2]Max-Delbrück-Center for Molecular Medicine, Berlin, Germany; [3]Institute for Translational Cancer Research and Experimental Cancer Therapy, Technical University Munich, Munich, Germany; [4]Department of General, Visceral and Pediatric Surgery, University Medical Center Göttingen, Göttingen, Germany; [5]Institute for Tumor Biology and Experimental Therapy, German Center for Translational Cancer Research (DKTK), Partner Site Frankfurt/Mainz, Georg-Speyer-Haus, Frankfurt, Germany; [6]German Cancer Research Center (DKFZ), Heidelberg, Germany; [7]Institute of Pathology, University Medical Center Göttingen, Göttingen, Germany; [8]Department of Gastroenterology, Gastrointestinal Oncology and Endocrinology, University Medical Center Göttingen, Göttingen, Germany; [9]CCC-N (Comprehensive Cancer Center Lower Saxony), Göttingen, Germany; [10]Clinical Research Unit 5002, KFO5002, University Medical Center Göttingen, Göttingen, Germany; [11]Max Delbrück Center for Molecular Medicine, Berlin, Germany; [12]Core Unit Proteomics, Berlin Institute of Health at Charité - Universitätsmedizin Berlin, Berlin, Germany; [13]EPO, Experimental Pharmacology and Oncology Berlin-Buch GmbH, Berlin, Germany; [14]Frankfurt Cancer Institute, Frankfurt, Germany; [15]German Center for Translational Cancer Research (DKTK), Partner Site Munich, Munich, Germany; [16]Institute of Diagnostic Laboratory Medicine, Clinical Chemistry and Pathobiochemistry, Charité - Universitätsmedizin Berlin, corporate member of Freie Universität Berlin and Humboldt-Universität zu Berlin, Berlin, Germany; [17]Cluster of Excellence ImmunoPreCept, Berlin, Germany; and [18]German Center for Translational Cancer Research (DKTK), Partner Site Berlin, Berlin, Germany

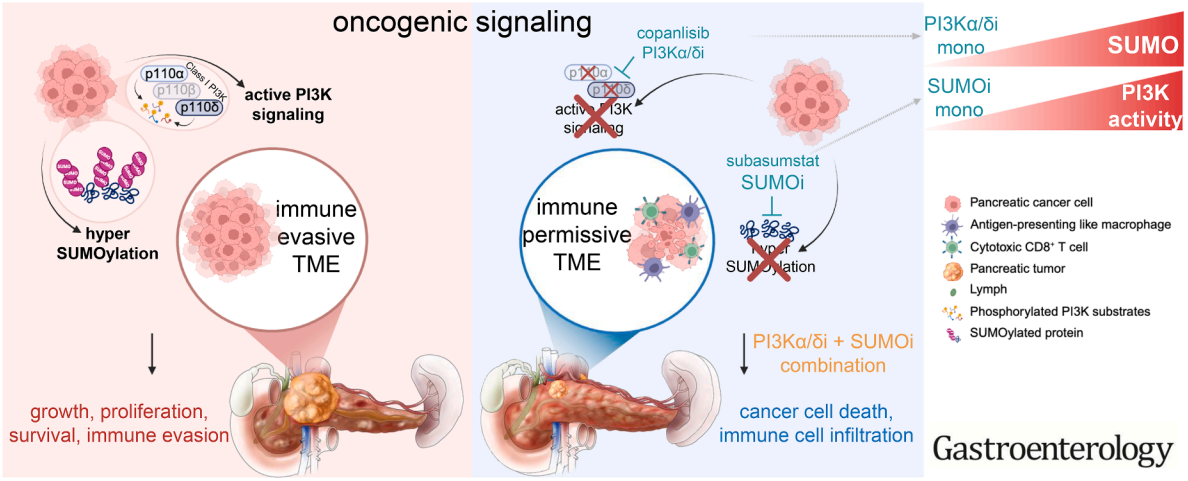

BACKGROUND & AIMS: Pancreatic ductal adenocarcinoma (PDAC) is a highly aggressive and lethal cancer, with a 5-year survival rate of <13%. Despite advances in diagnostics and treatments, the standard of care for PDAC remains inadequate, and most patients develop resistance to therapy. Targeted approaches, such as Kirsten rat sarcoma (KRAS) inhibition, have shown promise in preclinical models, although clinical application remains challenged by the rapid development of resistance. The phosphatidylinositol-3-kinase (PI3K) signaling pathway is critical for PDAC development and maintenance, yet pharmacologic targeting has failed to yield significant clinical benefits. **METHODS:** To investigate the relationship

between the PI3K and small ubiquitin-like modifier (SUMO) pathways in PDAC, we used a comprehensive approach that included unbiased genome-wide clustered regularly interspaced short palindromic repeats/clustered regularly interspaced short palindromic repeats-associated protein 9 resistance screens, pharmacologic screens, transcriptomics, proteomics, and phosphoproteomics experiments. Genetic knockout models were applied to validate our findings. A novel molecularly targeted combination therapy was tested in preclinical mouse models. **RESULTS:** Using genetic and pharmacologic screenings, we discovered a mutual and targetable codependence between the PI3K and the SUMO pathways. Simultaneous inhibition of PIK3α and PIK3δ, combined with SUMO-activating E1 targeting, triggered synthetic lethality and cell death. In syngeneic orthotopic immune-competent PDAC models, this combination therapy reduced tumor growth and promoted immune cell infiltration and activity. **CONCLUSIONS:** Our study introduces a novel rational combination therapy in PDAC. Dual targeting of PI3Kα/δ and SUMO signaling bears potential for clinical translation.

Keywords: Pancreatic Cancer; PI3K; SUMOylation; Regulated Cell Death; Combination Therapy.

Pancreatic ductal adenocarcinoma (PDAC) is one of the most aggressive and deadliest cancers, with a 5-year survival rate of just 13%. Despite its increasing incidence, including in younger patients, treatment options for PDAC remain limited and nonsatisfying.[1] PDAC is defined by a distinct genetic landscape, with frequent mutations in *KRAS*, *TP53*, *CDKN2A*, and *SMAD4*.[2] Activating *KRAS* mutations, present in 90% of cases, position the Kirsten rat sarcoma virus (KRAS)/mitogen-activated protein kinase signaling pathway as a central driver of tumor progression and a critical therapeutic target. Consequently, the recently developed rat sarcoma (RAS) inhibitors, including mutant-selective and pan-RAS inhibitors, have demonstrated promising early signs of clinical efficacy in PDAC.[3] However, genetic and adaptive resistance to RAS inhibition remains challenging,[3] underscoring the need of additional molecular targeted treatment strategies.

The phosphatidylinositol-3-kinase-(PI3K)–protein kinase B (AKT)–mechanistic target of rapamycin pathway has recently been implicated in resistance to RAS inhibitors.[4] Furthermore, the finding that oncogenic PI3K-signaling can compensate KRAS-dependency to initiate and drive carcinogenesis and tumor progression in murine PDAC models[5,6] highlights the PI3K pathway's significance as a therapeutic target. PI3K family kinases include 3 classes. Class Ia (p110α/PIK3CA, p110β/PIK3CB, and p110δ/PIK3CD) and class Ib (p110γ/PIK3CG) catalytic subunits are particularly relevant in clinical settings, with inhibitors targeting these isoforms available.[7] *PIK3CA* mutations are the most common alterations within class I PI3Ks and may predict sensitivity to PI3K inhibition in preclinical PDAC models.[7–9] Moreover, several isoform-specific PI3K inhibitors have been evaluated in clinical trials for solid tumors, including PDAC. Alpelisib (BYL-719), a PI3Kα inhibitor (NCT02155088,

WHAT YOU NEED TO KNOW

BACKGROUND AND CONTEXT

Resistance to therapeutic interventions for pancreatic ductal adenocarcinoma remains challenging. Phosphatidylinositol-3-kinase signaling is critical for pancreatic ductal adenocarcinoma maintenance and progression, but pharmacologic targeting has failed to yield significant clinical benefits.

NEW FINDINGS

Simultaneous inhibition of phosphatidylinositol-3-kinase α/δ, combined with small ubiquitin-like modifier-activating E1 targeting, triggered synthetic lethality. In syngeneic immune-competent pancreatic ductal adenocarcinoma models, this combination therapy reduced tumor growth and promoted immune cell infiltration.

LIMITATIONS

Combining phosphatidylinositol-3-kinase α/δ and small ubiquitin-like modifier inhibitors triggered an immune-assisted anti-tumor response, marked by an unexpected immunophenotype, a phenomenon that requires further investigation in future studies.

CLINICAL RESEARCH RELEVANCE

The dual targeting of phosphatidylinositol-3-kinase α/δ and small ubiquitin-like modifier shows efficacy, manageable toxicity in mice and potential for clinical translation in pancreatic ductal adenocarcinoma, a cancer with significant unmet medical needs.

BASIC RESEARCH RELEVANCE

Blockade of the phosphatidylinositol-3-kinase pathway leads to the adaptive activation of the small ubiquitin-like modifier (SUMO)ylation machinery and vice versa. Only the combined inhibition of both phosphatidylinositol-3-kinase α and δ with a clinical-grade E1 small ubiquitin-like modifier inhibitor induced synergistic cell death in vitro and demonstrated synergy in an immunocompetent in vivo model. Our work highlights the unexpected requirement of phosphatidylinositol-3-kinase α and δ in the small ubiquitin-like modifier–ylation-associated stress response.

[§] Authors share co-senior authorship.

Abbreviations used in this paper: **AKT, protein kinase B; Cas, clustered regularly interspaced short palindromic repeats-associated; CD, cluster of differentiation; CRISPR, clustered regularly interspaced short palindromic repeats; cycIF, cyclic immunofluorescence; GSEA, gene set enrichment analysis; KRAS, Kirsten rat sarcoma viral oncogene homologue; MYC, myelocytomatosis oncogene; PDAC, pancreatic ductal adenocarcinoma; PDO, patient-derived organoid; PI3K, phosphatidylinositol-3-kinase; PI3Ki, phosphatidylinositol-3-kinase inhibitor; RAS, rat sarcoma; RCD, regulated cell death; RNAseq, RNA sequencing; SAE1, small ubiquitin-like modified-activating enzyme subunit 1; snRNA, single nuclei RNA; SOC, standard of care; SUMO, small ubiquitin-like modifier; SUMOi, small ubiquitin-like modifier E1 inhibitor; TME, tumor microenvironment.**

0016-5085
https://doi.org/10.1053/j.gastro.2025.08.018

NCT02437318), has demonstrated tolerability in PDAC patients and efficacy in *PIK3CA*-mutated breast cancer.[10] GSK2636771, a PI3Kβ inhibitor, is currently under investigation (NCT04439188) in patients with *PTEN* loss.[11] Eganelisib (IPI549), targeting PI3Kγ (NCT02637531), has shown immune-modulation and antitumor activity when combined with nivolumab in solid tumors.[12] In contrast, idelalisib (CAL-101) and parsaclisib (INCB050465), both targeting PI3Kδ (NCT02468557, NCT02559492), have exhibited limited efficacy in solid tumors.[13,14] These findings highlight the clinical potential of isoform-specific PI3K inhibitors; however, their role and targeting spectrum in the treatment of PDAC has yet to be established.

The small ubiquitin-like modifier (SUMO)ylation signaling pathway is a cellular process in which SUMOs are attached to target proteins, altering their function, stability, or localization. SUMOylation plays a crucial role in regulating processes such as transcription, DNA repair, the cell cycle, and stress responses.[15] Pharmacologic targeting of the SUMO pathway has shown efficacy in PDAC and other malignancies in preclinical models.[16,17]

To harness the therapeutic potential of PI3K-pathway inhibition in PDAC, we investigated pathway co-dependencies to inform translational strategies. We observed that blockade of the PI3K pathway leads to the adaptive activation of the SUMOylation machinery and furthermore observed a vice versa process. Only the combined inhibition of both PI3Kα and PI3Kδ with a clinical-grade SUMO-inhibitor induced synergistic cell death in vitro and demonstrated synergy in an immunocompetent in vivo model. Our work highlights the unexpected requirement of PI3Kα and PI3Kδ in the SUMO-associated stress response and unveils a novel combination therapy approach with the potential for clinical applicability.

Methods

Pharmacologic Screen

The drug library consisting of $\geq$99 inhibitors targeting various relevant cancer pathways in PDAC was purchased from Selleckchem. Subastumstat was kindly gifted by Takeda. Copanlisib (cat no HY-15346R) and pictilisib (cat no HY-50094) were purchased from MedChemExpress LLC. The drug screen was conducted in MiaPaCa-2, PSN-1, and 53631PPT cells, as recently described.[18] After 72 hours of treatment, viability was measured. Plates were incubated at room temperature for 30 minutes 25 μL of CellTiter-Glo (Promega) was added to each well, incubated for 15 minutes, and luminescence was measured (FLUOstar-OPTIMA-microplate-reader, BMG-Labtech). Area under the curve and half-maximal growth inhibitory concentration values were calculated with RStudio (Posit Software) using a GRmetrics script.

Western Blot

Cells were treated with various conditions and harvested at different time points, and their protein lysates were analyzed by Western blot using specific primary antibodies and horseradish peroxidase–conjugated secondary antibodies. The blots were developed using the OdysseyM imager (LI-COR Biotech), and the data were analyzed using EmpiriaStudio software (LI-COR Biotech).

Growth Curves by Cell-Live Imaging

Cells were seeded onto 96-well plates (5×10^3 cells/well), grown for 24 hours, and then treated with the indicated compounds. Confluency was determined by monitoring cells in real time with a confluency image mask, which was filtered for each cell line specifically. Cell confluency was quantified by 2024A version of the Incucyte software.

CRISPR/Cas9-based Gene Editing

Depletion of *PI3Kα* a fragment from exon-2 and depletion of *PI3Kδ* from exon-3 was mediated by clustered regularly interspaced short palindromic repeat (CRISPR)/clustered regularly interspaced short palindromic repeat associated protein 9 (Cas9). Then, 150,000 cells were transfected with 500 ng of single-guide (sg)RNA and 1 μg of Cas9 protein (PNA-Bio) with a Neon-Transfection-System (Thermo Fisher/Invitrogen). A list of single-guide RNA sequences is available in the Supplementary Material and Methods. Cleavage efficacy was tested 72 hours after transfection with Terra PCR Direct Card Kit (Takara Bio). Single cells were generated by serial dilution. Clones were screened for efficient gene editing, and selected clones were analyzed for protein expression by immunoblotting.

In Situ Resistance Assay

Cells were seeded onto a 96-well plate at a density of 250 cells/well on day 0. On day 1, treatment was added. Medium was changed and drugs refreshed weekly. Each week, cell confluency was analyzed using Incucyte (Live-Cell Imager, Sartorius). Wells reaching >50% confluency were scored as resistant. Data were plotted as a Kaplan-Meier plot.[19]

Toxicity Analysis in Mice

Serum samples of mice were isolated by postmortem cardiac puncture centrifuged at 2000*g* for 10 minutes. The concentrations of lactate dehydrogenase activity, albumin, calcium, urea, total protein, bilirubin, alanine aminotransferase, aspartate aminotransferase, alkaline phosphate, and inorganic phosphate were analyzed by photometry on a Roche cobas analyzer (Roche Diagnostics, Rotkreuz, Switzerland).

Detailed information on single-nuclei (sn)RNA sequencing (seq), RNAseq, processing, and analysis of gene expression data; CRISPR/Cas9-knockout screen; cell culture and treatment, chemicals, viral infection, and colony formation assay; cyclic immunofluorescence; in vivo drug efficacy analysis in mice and immunohistochemistry; patient-derived organoids; global and phosphoproteomics; and flow cytometry is available in the Supplementary Material.

Statistics

Statistical analyses were performed using GraphPad Prism (GraphPad Software). P values <.05 were considered significant. All P values and tests are indicated in the figure legends.

Results

The SUMOylation Pathway Is Activated by PI3K Inhibition

PI3K-signaling is considerably involved in therapy resistance in multiple tumor entities.[20–22] In PDAC, catalytical class-I PI3-kinase expression is increased (Supplementary Figure 1*A*). Both basal-like and mesenchymal subtypes, which overlap and are known to be more resistant to chemotherapy,[23] exhibit elevated PI3K/AKT-pathway activity, although mutations are rarely found (Figure 1*A* and *B*[24] and Supplementary Figure 1*A* and *B*). Mining data of patient-derived organoids (PDOs) isolated from treatment-naive patients and patients after standard-of-care (SOC) chemotherapy[25] revealed a significant enrichment of the PI3K/AKT-signaling signatures in SOC-treated PDAC patients (Figure 1*C*). Furthermore, *KRAS*-knockout PDAC cells exhibited activated PI3K-dependent mitogen-activated protein kinase signaling and were sensitive to PI3K inhibition (Supplementary Figure 1*C*).[26] The combination of KRAS-inhibition by RMC-6236, a multiselective RAS^{on} inhibitor, and PI3K inhibition by pictilisib (a PIK3α/δ inhibitor) acted synergistic in selected PDAC cell lines (Supplementary Figure 1*D*). Together, these data highlight the critical role of PI3K-dependent rewiring of oncogenic networks in cells with perturbed KRAS. Therefore, specifically in the context of PDAC, PI3K signaling plays a crucial role in adaptation to therapy and in treatment resistance.

To gain a deeper understanding of PI3K-controlled molecular networks, we analyzed a $CRISPR^{knockout}$-based PI3K-inhibitor (pictilisib) resistance screen[27] and identified SUMOylation-related pathways as synthetic lethal (Figure 1*D*). To causally test the relationship between PIK3-inhibition and changes in SUMOylation, we investigated the course of global protein SUMOylation upon PIK3 inhibition with the formerly United States Food and Drug Administration–approved PIK3α/δ inhibitor copanlisib. Indeed, over time, PI3K inhibition induced protein SUMOylation (Figure 1*E* and Supplementary Figure 1*E*), pointing to a role of SUMO in cells with inactivated PI3K signaling.

To extend our findings, we generated PI3K-inhibitor (copanlisib)–resistant PDAC cells (PI3K-R) and identified the induction of the SUMO-pathway core components SUMO1, SUMO2, SUMO3, and SUMO-activating enzyme subunit 1 (SAE1), ubiquitin-like modifier activating enzyme 2 (UBA2), and UBE2I (Figure 1*F* and Supplementary Figure 1*E*). We also examined the SUMOylation status after application of several selected SOC or targeted compounds. We observed induction of SUMOylation in some treatments, but not a general SUMO induction (Supplementary Figure 1*F*).

We next evaluated SUMOylation induction in PI3K inhibitor–treated MiaPaCa-2 by proteomics and phosphoproteomics (Figure 1*G*). Here, we found a significant induction of SUMO1 after 6 hours and SUMO2 after 24 hours (Figure 1*H*) upon PI3K inhibition. Additionally, various SUMOylation-related signatures were induced already after 6 hours, with some sustained after 24 hours (Figure 1*I*), indicating early changes of protein SUMOylation in PI3K-inhibited cells. Sentrin/SUMO-specific proteases, which contribute to the maturation and homeostasis of SUMOylated proteins,[28] also showed a tendency toward induction after PI3K inhibition, with the SUMO2/3-specific deSUMOylase sentrin/SUMO-specific protease 3 being induced in particular (Supplementary Figure 1*G*). Phosphoproteomics and immunoblotting confirmed efficacy of PI3K inhibitor treatment as indicated by reduced phosphorylation of downstream targets (Figure 1*J* and Supplementary Figure 1*H*).

Together, these data show the induction of SUMOylation upon blockade of the PI3K pathway. Considering the synthetic lethal relation detected in the CRISPR screen (Figure 1*D*), the activation of SUMOylation pointed toward a functional relevance for PDAC cell survival.

SUMOylation Inhibition Induces PI3K Dependence

Observing the activation of SUMOylation in response to PI3K inhibition and in patients receiving SOC (Supplementary Figure 1*I* and *J*), we next sought to identify global PDAC dependencies in the context of SUMO pathway targeting. To this end we applied the highly specific clinical-grade SUMO E1 inhibitor (SUMOi) subasumstat[29] in a genome-wide CRISPR-knockout resistance screening in MiaPaCa-2 and PSN1 (Figure 2*A*). Indeed, we revealed that loss of genes associated with the PI3K/AKT pathway exhibited significant synthetic lethality in the context of SUMO blockade (Figure 2*B* and Supplementary Table 1). Complementary to the forward-directed genetic screen, we performed a subasumstat-anchored pharmacologic screen in human (MiaPaCa-2 and PSN1) and murine 53631PPT PDAC cell lines (Supplementary Table 2). Again, we identified a synthetic lethal relation between the SUMO and PI3K pathways (Figure 2*C*), which could be validated by multidose treatment with subasumstat (Figure 2*D*). In sum, these findings pointed toward a potential codependence of the 2 pathways in PDAC.

Pictilisib and copanlisib both exhibit equipotent inhibition of PIK3α and PIK3δ and less potent inhibition of PIK3β and PIK3γ isoforms.[30,31] Owing to the ample (pre)clinical data, including some efficacy as well as toxicity and tolerability from clinical studies in lymphoma[32] and other cancer entities,[33] we focused further studies on the formerly Food and Drug Administration-approved compound copanlisib. Combined treatment with copanlisib and subasumstat proved a targetable codependence between both pathways (Figure 2*E* and *F*). The synergistic effects of combined PI3K/SUMO targeting were confirmed in an expanded panel of PDAC cell lines (Supplementary Figure 2).

Taken together, these data indicate that SUMOylation inhibition provoked a cellular dependency on PI3K signaling. PI3K signaling thus represents a convergent node and specific vulnerability in PDAC cells lacking a functional SUMOylation machinery, and vice versa.

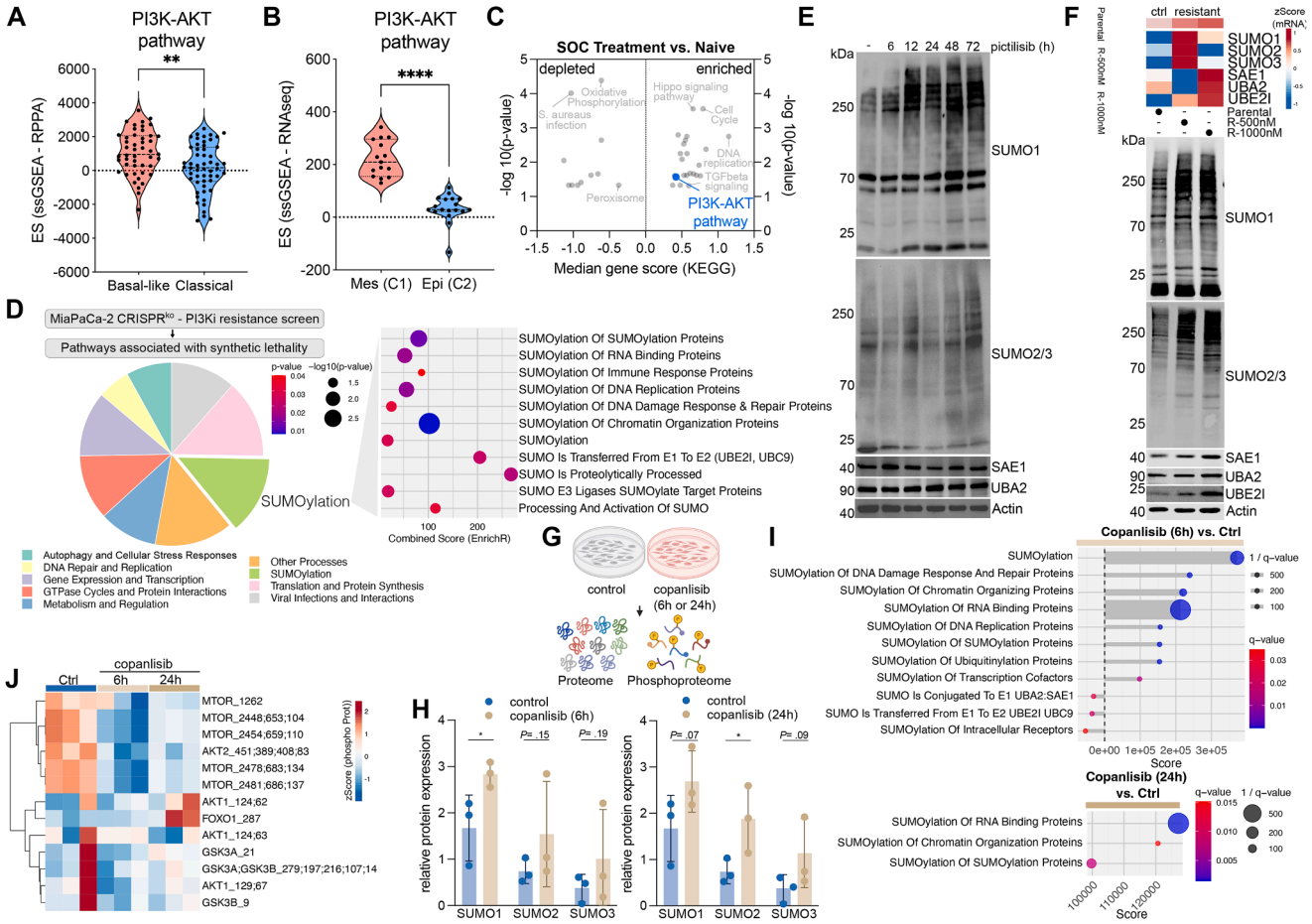

Figure 1. SUMOylation is enriched upon PI3K targeting in PDAC. (*A*) Distribution of single-sample (ss)GSEA enrichment scores for proteins of the Kyoto Encyclopedia of Genes and Genomes (KEGG) PI3K-AKT pathway in indicated PDAC subtypes. The *large dashed lines* inside the violin plot indicate the median and the *smaller dashed lines* indicate the interquartile range. (RPPA, Reverse Phase Protein Array, The Cancer Genome Atlas database). $^{**}P < .01$ by *t* test. (*B*). Distribution of ssGSEA enrichment score for messenger RNA of the KEGG PI3K-AKT pathway in mesenchymal (mes) C1 and epithelial (epi) C2 murine PDAC subtypes.[24] $^{****}P < .0001$ by *t* test. (*C*) Top KEGG pathways enriched in post-chemotherapy PDOs shows an up-regulation of the PI3K-AKT pathway upon treatment.[25] TGF, transforming growth factor. (*D*) Results from genome wide CRISPR-knockout PI3K-inhibition resistance screen performed in MiaPaCa-2.[27] GSEA analysis (Reactome) of negatively selected genes revealed a synthetic lethal interaction between PI3K inhibition and SUMOylation inhibition. GTPase, guanosine-5′-triphosphatases. (*E*) Immunoblot analysis shows indicated proteins upon PI3K inhibition with pictilisib (1000 nmol/L) in MiaPaCa-2 for indicated time points. β-Actin served as the loading control. UBA2, ubiquitin-like modifier activating enzyme 2. (*F*) *Top*: Transcript levels SUMO core components of MiaPaCa-2 cells—parental and resistant to copanlisib (R-500 nmol/L; R-1000 nmol/L). UBE2, ubiquitin-conjugating enzyme E2. *Bottom*: Immunoblot of SUMO core components in copanlisib resistant (R-500 nmol/L; R-1000 nmol/L) and parental MiaPaCa-2 cells. (*G*) Illustration of the global- and phosphoproteomics experimental setup. MiaPaCa-2 cells were treated for 6 or 24 hours with copanlisib (1000 nmol/L) or treated with dimethyl sulfoxide (vehicle-control). (*H*) Relative SUMO1/2/3 protein expression upon PI3K inhibition with copanlisib (1000 nmol/L, 6 or 24 hours; n = 3). *P* value by *t* test as indicated or $^{*}P < .05$. The *range bars* designate standard deviation. (*I*) GSEA of SUMOylation-related gene sets (Reactome) upon PI3K inhibition with copanlisib (1000 nmol/L) for 6 or 24 hours compared with vehicle/ dimethyl sulfoxide control in MiaPaCa-2. (*J*) Phosphorylation of indicated PI3K-Akt-mechanistic target of rapamycin (MTOR) downstream targets (mass spectrometry) upon PI3K-inhibition with copanlisib (1000 nmol/L) for 6 or 24 hours compared with vehicle/ dimethyl sulfoxide control (MiaPaCa-2). GSKA, glycogen synthase kinase-3 alpha; FOXO1, forkhead box protein O1.

Simultaneous Inhibition of PIK3α/δ and SUMO Is Required to Induce Synthetic Lethality

Our data indicate that inhibition of PIK3α and PIK3δ effectively induced susceptibility to SUMOylation inhibition, a crucial finding for clinical translation. To further corroborate the dependency on specific PI3K isoforms and to provide robust data vital for clinical translation, we directly tested various PI3K inhibitors with known specificities for individual PI3K isoforms: alpelisib (PI3Kα),[10] GSK2636771 (PI3Kβ),[11] eganelisib (PI3Kγ),[12] idelalisib

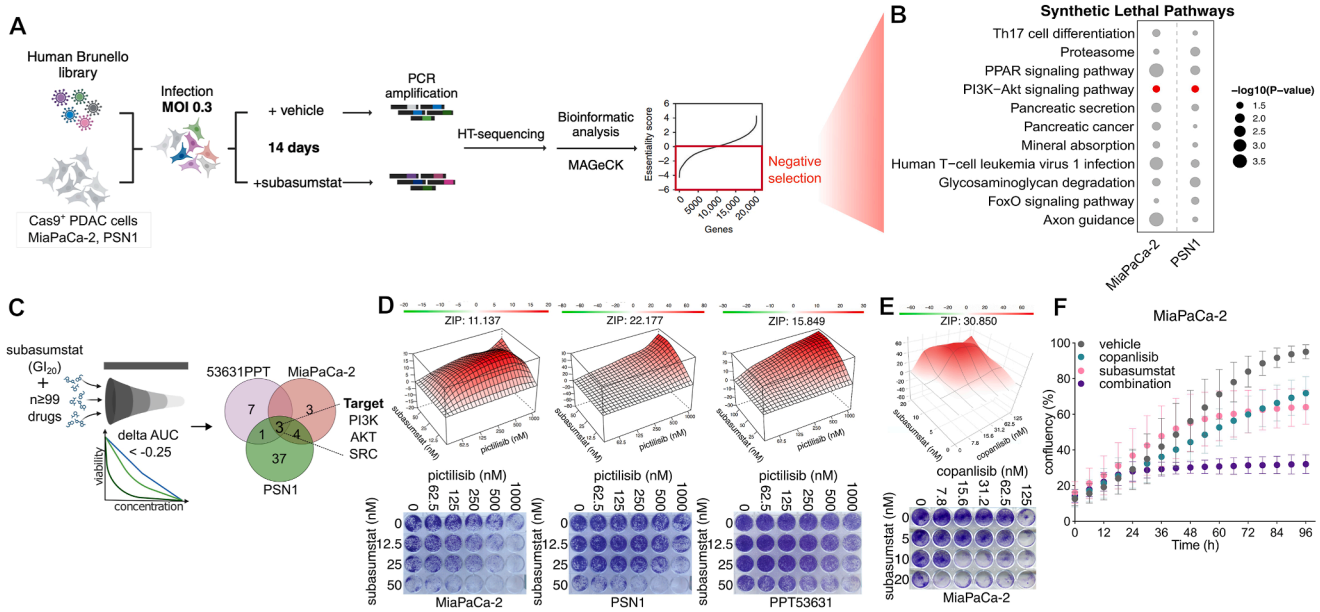

Figure 2. Synthetic lethal interaction between SUMO and PI3K pathways. (*A*) Schematic overview of the genome-wide CRISPR/Cas9 knockout subasumstat-resistance screen strategy conducted in MiaPaCa-2 and PSN1. HT, high throughput; MAGeCK, Model-based Analysis of Genome-wide CRISPR/Cas9 Knockout; MOI, multiplicity of infection; PCR, polymerase chain reaction. (*B*) Kyoto Encyclopedia of Genes and Genomes (KEGG) pathway analysis of negatively selected genes from CRISPR^{knockout} screens in the MiaPaCa-2 and PSN1 exposes the PI3K-Akt pathway as a common synthetic lethal pathway. PPAR, peroxisome proliferator–activated receptors; Th17, T helper 17. (*C*) Illustration/results of the subasumstat-anchored pharmacologic screen setup of subasumstat 20% growth inhibitory concentration (GI_{20}) and multidose treatment of n $\geq$ 99 compounds indicating in 3 indicated cell lines. AUC, area under the curve. (*D*) *Top*: Landscape plots depicting the synergistic area of concentrations of subasumstat and the PI3K inhibitor (pictilisib) in the 3 PDAC indicated cell lines. Synergy score was determined by SynergyFinder using the Zero Interaction Potency (ZIP) method. *Bottom*: Representative colony-growth images after treatment with subasumstat and pictilisib. (*E*) *Top*: Landscape plot depicting the synergistic area of concentrations of subasumstat and copanlisib in MiaPaCa-2. *Bottom*: Representative colony-growth image after treatment with subasumstat and copanlisib. (*F*) Proliferation of MiaPaCa-2 supplemented with subasumstat, copanlisib, or the combination of both. Cell confluency data were obtained by live cell imaging (n = 3). The *range bars* designate standard deviation.

(PI3Kδ),[34] and parsaclisib (PI3Kδ),[14] all in combination with subasumstat. None of the isoform-specific PI3K inhibitors displayed synergism with subasumstat (Figure 3*A* and *B*, Supplementary Figure 3*A*). To substantiate these findings, we performed genetic knockouts of *PIK3α* or *PI3Kδ* isoforms by CRSIPR/Cas9 (Figure 3*C* and Supplementary Figure 3*B*). Single knockout of the *PIK3α* or *PI3Kδ* isoforms did not exhibit synergism under subasumstat treatment. However, treating *PI3Kα* knockout cells with a PI3Kδ-specific inhibitor displayed synthetic lethality with the SUMOi subasumstat (Figure 3*D* and *E*). Confirming our previous data on SUMO pathway activation upon pharmacological PI3K-targeting (Figure 1) and supporting the codependence of the 2 pathways and in particular the specific PI3K isoforms, the SUMO state was increased in p110δ/PI3Kδ and p110α/PI3Kα knockout cells (Figure 3*F*, and Supplementary Figure 3*B*). In parental cells, the induction of a polySUMOylation high state upon PIK3α/δ inhibition was blocked upon combination with subasumstat (Supplementary Figure 3*C*).

Together, these results show that highly specific PI3Kα/δ inhibition or loss of PI3Kα/δ induced profound activation of protein SUMOylation and created a targetable vulnerability. Consequently, inhibition of specifically PI3Kα/δ is required and sufficient for optimal synergy with SUMO-targeting by subasumstat.

Combined PI3Kα/δ–SUMO Inhibition Induces Regulated Cell Death in Pancreatic Ductal Adenocarcinoma

To identify relevant pathways responsible for the fate of PDAC cells upon dual PI3K and SUMO inhibition, we examined the transcriptome and (phospho-)proteome upon monotreatment and combination treatment with copanlisib and subasumstat (Figure 4*A*). Single-sample gene set enrichment analysis (GSEA) revealed distinct patterns in the transcriptome (Figure 4*B*) and proteome (Figure 4*C*). PI3K signaling was significantly reduced and myelocytomatosis oncogene (MYC) signatures were depleted in both copanlisib monotherapy and combination with subasumstat, consistent with earlier observations.[35,36] By analyzing hallmark signatures of the molecular signature database (MSigDb) enriched in the transcriptome and the proteome in the combination treatment, we identified 6 overlapping signatures, including metabolic, heme metabolism, and apoptosis signatures (Figure 4*D*). Therefore, we analyzed the expression of proteins related to apoptosis

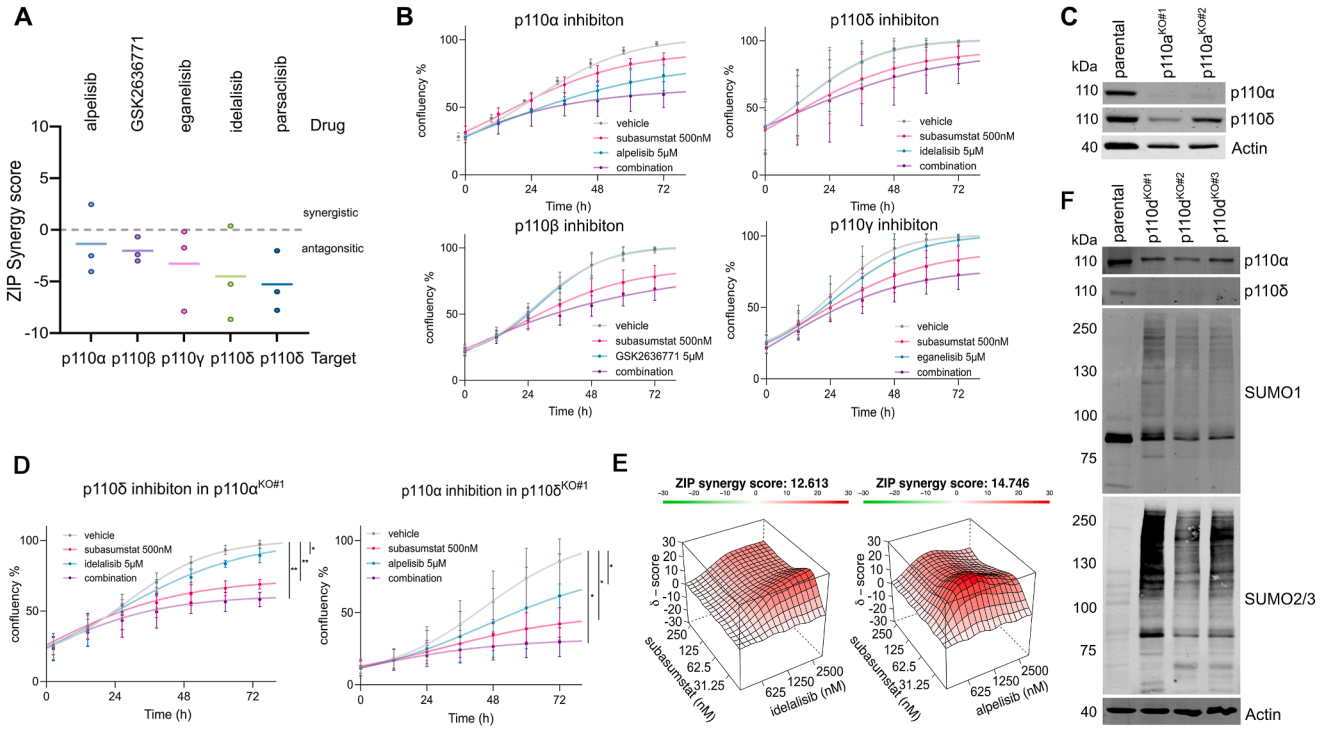

Figure 3. Double targeting of PI3Kα/PI3Kδ and SUMOylation induces synthetic interaction. (*A*). Zero Interaction Potency (ZIP) synergy scores upon combination of subasumstat and indicated PI3K inhibitors in MiaPaCa-2. Cells were treated with single and combination treatments using a 4 × 5 matrix. Cell confluency was assessed after 96 hours, and clonogenic assay quantification was imaged. Synergy score was determined by SynergyFinder using the ZIP method (n = 3). (*B*) Proliferation of MiaPaCa-2 supplemented with 500 nmol/L subasumstat, 5 μmol/L of indicated PI3K-specific inhibitors, or the combination of both. Cell confluency data were obtained by live cell imaging (12-hour intervals over 72 hours; n = 3). The *range bars* designate standard deviation. (*C*) Immunoblot analysis of p110α/δ expression in MiaPaCa-2 harboring a CRISPR/Cas9-mediated PI3Kα-de(p)letion. (*D*) Proliferation of p110α-depleted MiaPaCa-2 supplemented with 500 nmol/L subasumstat, 5 μmol/L idelalisib, or the combination (*left*), and p110δ-depleted MiaPaCa-2 supplemented with 500 nmol/L subasumstat, 5 μmol/L alpelisib, or the combination (*right*). Cell confluency data were obtained by live cell imaging (12-hour intervals over 72 hours; n = 3). $^{**}P < .01$ by analysis of variance. The *range bars* designate standard deviation. (*E*) Landscape plots depict the synergistic area of concentrations of idelalisib and subasumstat combination treatment in p110α-de(p)leted MiaPaCa-2 treated for 96 hours (*left*) and of concentrations of alpelisib and subasumstat combination treatment in p110δ-depleted MiaPaCa-2 treated for 96 hours (*right*). Data (n = 3) were obtained by confluency measurement. (*F*) Immunoblot analysis of indicated proteins in MiaPaCa-2 harboring a CRISPR/Cas9-mediated PI3Kδ-de(p)letion.

and other regulated cell death (RCD) modes (Figure 4*E*). Because we observed a trend for the regulation of proteins favoring apoptosis, we stained for cleaved caspase 3 and performed annexin-V/propidium iodide fluorescence-activated cell sorter. We observed an increase of cleaved caspase 3 (Supplementary Figure 4*A*) and annexin-V–positive cells upon combination treatment, which was blocked by a pan-caspase inhibitor (Figure 4*F*). However, the sole induction of apoptosis, which was relatively mild compared with the strong synergism observed, does not fully account for the cell-death mode. Analyses of cell-cycle profiles did not provide additional insights into the mode of action of the synergistic effects in the combination treatment (Supplementary Figure 4*B*). Considering the functional impact of SUMOylation on protein function and stability, we next investigated signatures and signaling pathways regulated at the protein level only. Applying phosphoproteomics, we identified that the SUMOi-PI3K inhibitor (PI3ki) combination specifically altered metabolic pathways, messenger RNA metabolism, and mitotic regulation (Figure 4*G*), suggesting that affecting such pathways contribute to the strong synergism.

In summary, these data identified a multimodal induction of RCD by the combined inhibition of the PI3Kα/δ and SUMOylation pathways.

Inhibition of PI3Kα/δ and SUMO Signaling Impairs Growth in Patient-Derived Organoids

To validate the efficacy of combined PI3Kα/δ-SUMO inhibition in advanced human model systems, we performed drug testing in 5 genetically and phenotypically characterized epithelial-like and mesenchymal-like PDOs with different activity of pathways associated with the mesenchymal subtype (Figure 5*A* and *B*). We tested their response toward FOLFIRINOX (folinic acid, fluorouracil, irinotecan, and oxaliplatin) (Figure 5*C*) and the PI3Kα/δ- and SUMO-inhibition (pictilisib/subasumstat) combination treatment (Figure 5*D*). Of note, PDOs associated with mesenchymal transcriptomic features

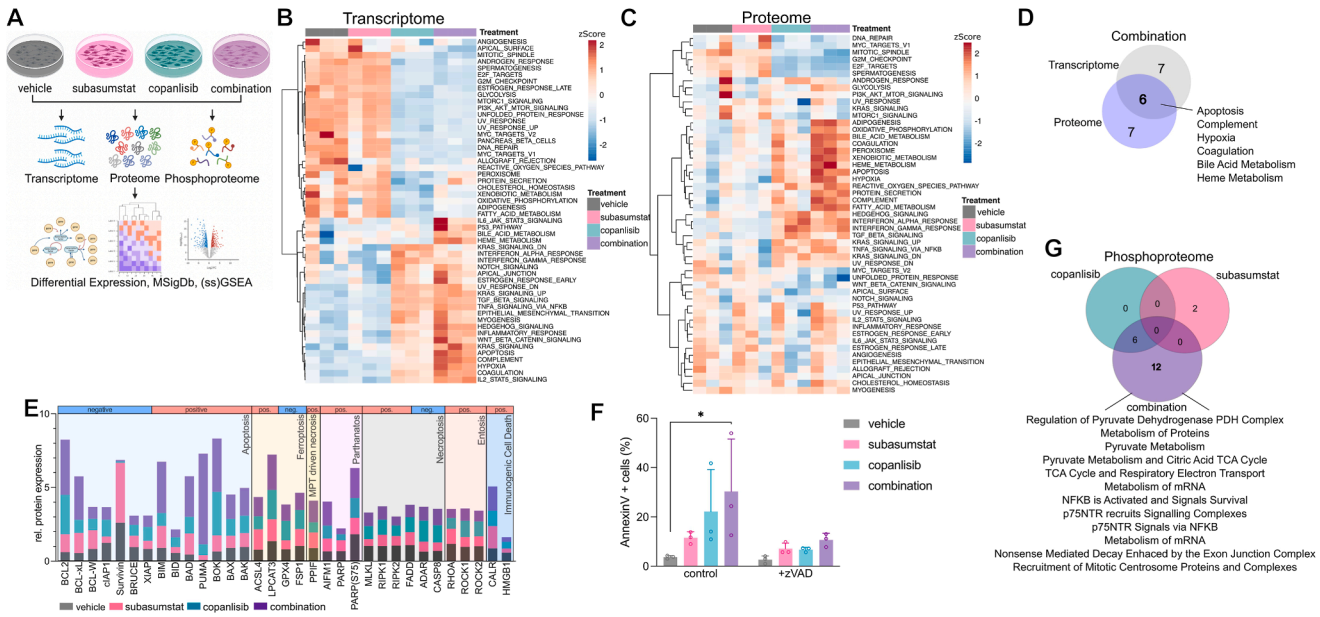

Figure 4. Multiomics analysis identifies an RCD-pattern in PDAC upon dual inhibition of PI3Kα/δ and SUMO. (*A*) Illustration of the experimental multiomics setup followed to elucidate the mechanistic effects of the single and combination treatments. Hallmark single-sample (ss)GSEA of (*B*) transcriptome and (*C*) proteome results upon treatment with subasumstat (200 nmol/L), copanlisib (1000 nmol/L), or the combination of both for 24 hours compared with vehicle/dimethyl sulfoxide (DMSO) control in MiaPaCa-2. (*D*) Top enriched overlapping gene sets of transcriptome and proteome analyses upon combination treatment. (*E*) Relative protein expression analysis of indicated forms of RCD in MiaPaCa-2 supplemented with DMSO, subasumstat (200 nmol/L), copanlisib (1000 nmol/L), or the combination for 24 hours. (*F*) Flow cytometry of propidium iodide/annexin-V staining of MiaPaCa-2 after subasumstat (200 nmol/L), copanlisib (1000 nmol/L), or combination treatment supplemented with zVAD-fmk (50 μmol/L) for 24 hours (n = 3). *$P < .05$ by analysis of variance. (*G*) Venn diagram overlapping the top enriched Reactome gene sets from indicated phosphoproteomes (n = 5, each condition). mRNA, messenger RNA; NFKB, nuclear factor κ-light-chain-enhancer of activated B cells; PDH, pyruvate dehydrogenase; TCA, tricarboxylic acid.

displayed poor response in the SOC treatment but an improved response in the pictilisib/subasumstat combination treatment compared with epithelial-like PDOs (Figure 5*C* and *D*). By GSEA we identified significant enrichments of SUMOylation signatures in responder PDOs associated with mesenchymal transcriptomic features (Figure 5*E*).

Next, we used in situ resistance assays[19] to assess viability after long-term treatment with monotherapy or combination therapy over a 5-week period. Outgrowth was defined on a confluence threshold of >50%, which was considered indicative of therapy failure. Cells treated with monotherapy exhibited outgrowth after 3 to 4 weeks, respectively (Figure 5*F*). In contrast, PI3Kα/δ-SUMOi combination therapy resulted in a pronounced loss of confluence, with >90% of cultures deemed nonviable by week 4 to 5 (Figure 5*F*).

In summary, the PI3Kα/δ-SUMO–targeted combination therapy demonstrated efficacy in PDOs and in long-term assays.

Combined PI3Kα/δ and SUMO Targeting Acts by Licensing the Antitumor Immune Response

We next investigated the PI3Kα/δi-SUMOi combination therapy in MiaPaCa-2 xenografts to translate our findings into an in vivo model. We observed a reduced tumor volume in combination-treated xenografts compared with monotherapy (Supplementary Figure 5).

Subasumstat treatment induced multifaceted immune effects.[17,37,38] Gene ontology biological process GSEA indicates up-regulated major histocompatibility complex-I and antigen processing and presentation upon combination treatment in MiaPaCa-2 (Figure 6*A* and *B*). Therefore, to investigate whether efficacy of combined PI3Kα/δ-SUMO was different in an immune-competent model and whether PI3Kα/δ-SUMO targeting could be associated with an antitumor response, we generated syngeneic orthotopic tumor grafts (Figure 6*C*). Here PI3Kα/δi-SUMOi treatment in a dose-escalation schedule exhibited significant effects on tumor growth compared with control treatments (Figure 6*D*). To investigate the effects of combined PI3Kα/δi-SUMOi treatment on tumor and immune dynamics, cyclic immunofluorescence (cycIF) was performed using the T-cell markers cluster of differentiation (CD) 3, CD4, CD8, and programmed cell death protein 1. This analysis revealed an increased infiltration of $CD3^+$ T cells (Figure 6*E*). Because we did not observe significant differences in $CD4^+$ or $CD8^+$ T-cell infiltration, immune histochemical analysis of $CD3^+$ T-cell infiltration was additionally performed, which confirmed the cycIF findings (Figure 6*F*).

Next, to investigate the complete landscape of therapy-induced reprogramming of the tumor microenvironment (TME), we analyzed tumor samples from all groups by

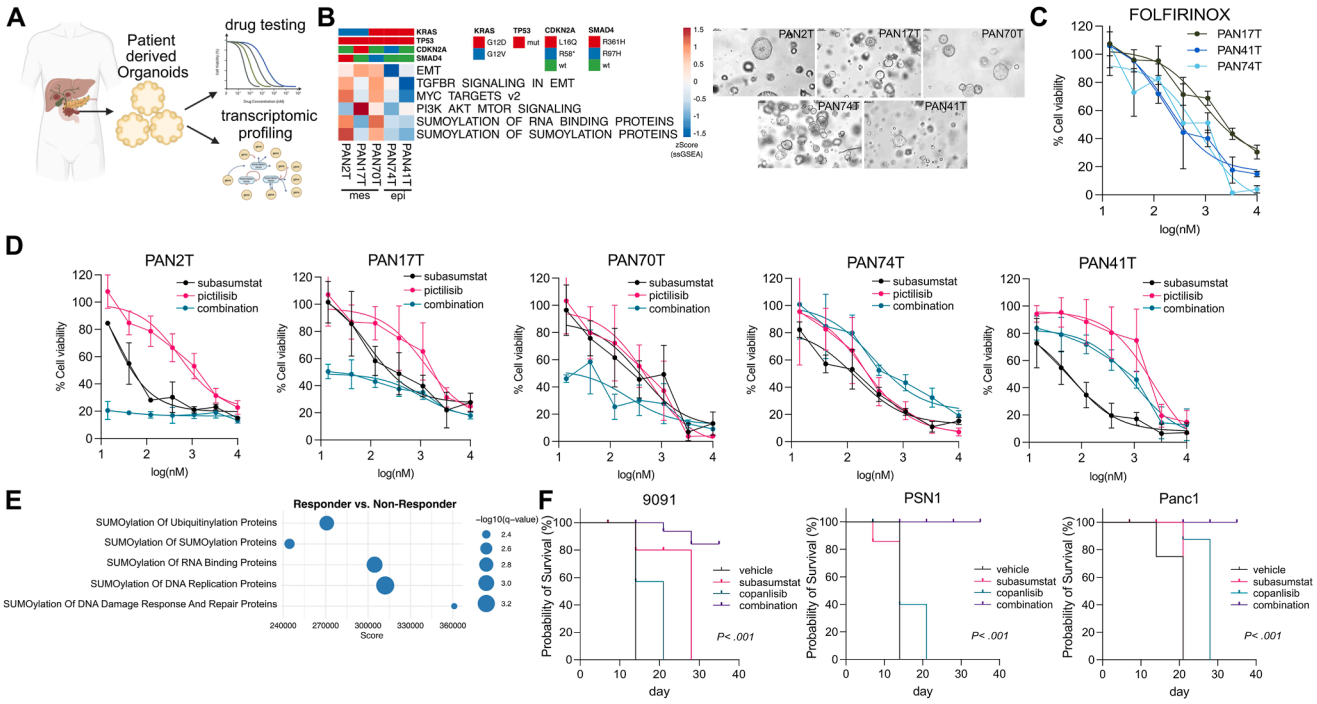

Figure 5. PDOs and in situ resistant assays reveal reduced tumor cell growth upon PI3Kα/δ and SUMO inhibition. (*A*) PDOs from 5 patients with PDAC were isolated and used for drug testing and transcriptomic profiling (schematic overview). (*B*) *Left*: Mutation status of *KRAS*, *CDKN2A*, *TP53*, and *SMAD4*, and GSEA of indicated PDOs. PAN2T, PAN17T, and PAN70T display mesenchymal-like features (mes); PAN41T and PAN74T display epithelial-like features (epi). *Right*: Representative phase-contrast images (similar magnification) of PDOs. EMT, epithelial-mesenchymal transition. (*C*) Cell viability, measured by adenosine triphosphate quantification (CellTiter-Glo) 96 hours after treatment with indicated concentrations of FOLFIRINOX (folinic acid, fluorouracil, irinotecan, and oxaliplatin) mes and epi PDOs (n = 3). (Original magnification, 20× objective.) (*D*) Cell viability of PDOs supplemented for 96 hours with subasumstat (10 nmol/L), pictilisib (indicated concentration), or the combination of both measured by adenosine triphosphate quantification (CellTiter-Glo) (n = 3). The *range bars* designate standard deviation. (*E*) GSEA (Reactome) of transcriptome data depicts increased SUMOylation signatures in mes-PDOs (responder), compared with nonresponding epi-PDOs. (*F*) In situ resistance assay in mesenchymal murine PDAC cell line 9091PPT and the 2 basal-like human PDAC cell lines PSN1 and Panc1. Log-rank *P* value is indicated.

snRNAseq (Figure 6*G* and Supplementary Figure 6*A* and *B*). Here, we observed increased expression of cycling and cytotoxic T cells, indicating T-cell activation, although surface CD8 detection may be reduced posttranscriptionally (Figure 6*G* and *H* and Supplementary Figure 6*C*). We found that PI3Kα/δi-SUMOi combination treatment significantly induced transcriptional activation of *Xcl1* and *Il18r1* in T cells, suggesting enhanced effector function (Figure 6*I*). In support, cycIF revealed a significant increase in $CD3^+CD8^+CCL5^+$ (chemokine ligand 5) and $CD3^+CD8^+Ki67^+$ cells, compatible with elevated cytotoxic activity and T-cell proliferation (Figure 6*J*). These findings point to a PI3Kα/δi-SUMOi combination-induced amplification of T-cell phenotypes associated with antitumor immunity.

Macrophage profiling revealed a shift from immunosuppressive M2-like macrophages to antigen-presenting tumor-associated macrophages (Figure 6*K* and *L* and Supplementary Figure 6*D*), compatible with a TME with enhanced antitumor immunity.[39] Additionally, cycIF showed up-regulation of chemokine ligand 5, a chemokine known to recruit effector T cells, natural killer cells, dendritic cells, and monocytes into the TME (Figure 6*M*).[40] In line with our cell culture–based data, we observed an augmented induction of interferon-α/γ and apoptosis pathways in tumor cells treated with the combination therapy in vivo (Supplementary Figure 6*E*).

Preliminary shallow analysis of toxicity regarding hematologic, liver, or kidney effects revealed no signals for PI3Kα/δi-SUMOi combination therapy in the investigated mouse cohorts (Supplementary Figure 7).

Together, these findings indicate that the combination therapy of SUMOi and PI3Kα/δi modulates the TME to favor immune-mediated tumor-cell killing, predominantly involving cytotoxic T cells and antigen-presenting macrophages.

Discussion

The analysis of genome-wide PI3Ki-CRISPR resistance screens[27] and our genome-wide SUMOi-CRISPR and drug screens led to the identification of PI3Kα/δ-SUMO targeting as a novel treatment strategy for PDAC. Our study reveals that mesenchymal/basal-like PDACs exhibit a mutual co-dependence on PI3K signaling and the SUMOylation pathway. By targeting both pathways, we achieved

consistent efficacy across multiple basal-like/mesenchymal models, including human and murine PDAC cell lines, PDOs, and mouse models, including an immune-proficient orthotopic model. Furthermore, our study underscores the importance of precise PI3K inhibitor application, because only PI3Kα/δ-inhibitors synergize with SUMOylation inhibitors.

Direct targeting PI3Ks is a treatment strategy in PDAC worth considering.[8] Our data confirm the connection between the PI3K pathway and basal-like/mesenchymal PDACs previously reported.[41] Importantly, PI3Kα is an important positive effector of oncogenic KRAS.[42] The interconnection of these 2 oncogenic signaling nodes is also evident in PDAC tumorigenesis, where PIK3α, but not

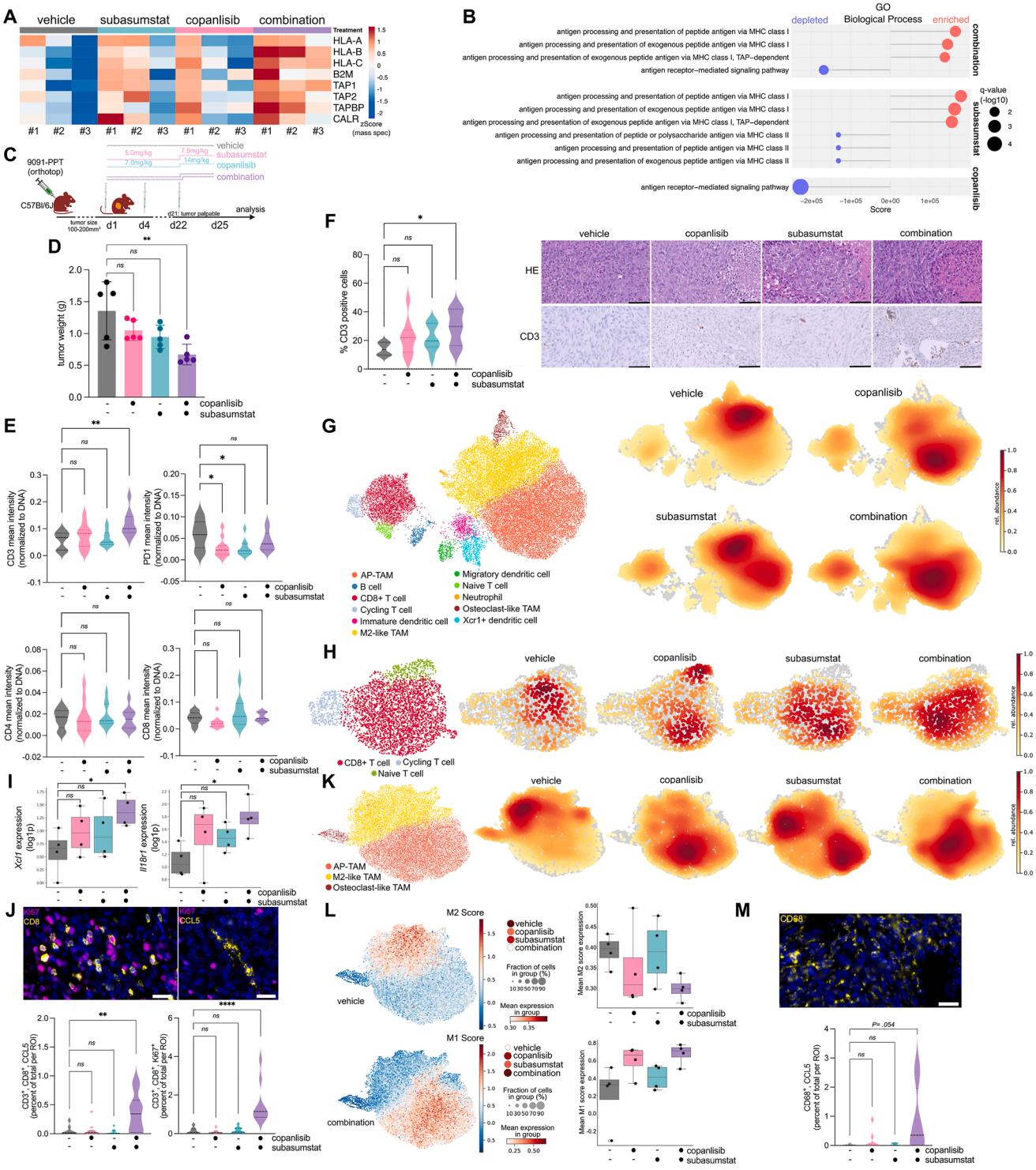

PIK3β, is an essential mediator of oncogenic KRAS signaling. Furthermore, oncogenic PIK3α is crucial for maintenance and metastatic progression of PDAC.[5,6,41,43,44] The observation that survival of PDAC cells genetically lacking KRAS is largely dependent on PI3K signaling[26] additionally emphasizes the pertinency of the PI3K pathway as a therapeutic target. In contrast to PI3Kα, the role of other class I PI3Ks in PDAC remains complex and is less well understood.

Immunohistochemistry demonstrated the expression of PI3Kγ in most of the investigated human PDAC cases, and knockout of the *PI3Kγ* gene delayed tumor development in murine PDAC models, involving nonautonomous mechanisms.[45–47] Furthermore, PDAC cells with mutated KRAS^{G12R}, which cannot interact with PI3Kα, overexpress and depend on PI3Kγ to induce micropinocytosis, a pathway that fuels the cancer cell's metabolic demands.[48] Protein abundance of PI3Kδ is up-regulated in tumor-enriched PDAC samples.[49] We demonstrate that the synergy of the SUMO and the PI3K pathway inhibition depend on specifically blocking PIK3α and PI3Kδ signaling. Thus, rational and specific inhibitor selection is needed to fully exploit PI3K inhibition in a specific context as shown here for the combination with SUMO targeting.

Recent studies by us and others have shown that the SUMOylation machinery is a putatively relevant therapeutic target in PDAC, and a highly potent and specific clinical grade SUMO E1 inhibitor has been evaluated in the clinic.[16,17,36] Concurrent with the activity of the PI3K pathway in basal-like PDACs, we observed increased expression of the core SUMOylation machinery in this subtype. The observed global/group protein SUMOylation upon PI3K inhibition appears consistent with cellular stress responses seen under conditions such as DNA damage or heat shock, where similar widespread SUMOylation shifts were identified.[50] This phenotype may reflect an adaptive or compensatory signaling mechanism engaged by cells to mitigate the disruption of homeostasis caused by PI3K pathway blockade. Our findings thus support the growing view that group SUMOylation plays a role in orchestrating broad stress-response programs, potentially as a protective means to buffer therapeutic stress.[51]

Importantly, inhibition of both the SUMO and the PI3K pathways resulted in activation of the other pathway, possibly as a mechanism to cope with various stresses, creating a therapeutically exploitable vulnerability and synthetic lethality. As shown previously, activation of SUMOylation confers a selective advantage against various stresses, contributing to cellular resilience against oncogenic, hypoxic, therapeutic, or oxidative stress.[52] Combined PI3K and SUMO inhibition induced multimodal effects and therapeutic synergism, with disruption of cell survival signaling and an RCD pattern reflecting features of oxidative stress-associated cell death.

Figure 6. Enhanced efficacy of combined subasumstat and copanlisib treatment in immunocompetent mice. (*A*) Analysis of mass spectrometry data from MiaPaCa-2 cells treated with subasumstat (200 nmol/L), copanlisib (1000 nmol/L), combination, or dimethyl sulfoxide as vehicle control (n = 3, each condition), reveals a significant induction of major histocompatibility complex (MHC)-I–associated proteins expression upon combination treatment. B2M, β_2 microglobulin; CALR, calreticulin; HLA, human leukocyte antigen; TAP, transporter associated with antigen processing; TAPBP, TAP binding protein. (*B*) GSEA (gene ontology [GO]/biological process) indicates up-regulated MHC-I and antigen processing and presentation upon combination treatment in MiaPaCa-2. (*C*) Experimental setup to investigate the combination treatment in orthotopic PDAC tumors (*D–M*). Mesenchymal 9091PPT cells were orthotopically transplanted. Mice were treated with vehicle, subasumstat, copanlisib, or the combination with the indicated schedule. (*D*) Tumor burden was measured over time and shows significantly decreased volume in response to combination therapy (n = 5 mice, each cohort). $^{**}P < .01$ by analysis of variance (ANOVA) with Tukey's post hoc test; ns, not significant. (*E*) Quantification of indicated markers normalized to DNA (4′,6-diamidino-2-phenylindole) show significantly increased CD3$^+$ T-cell infiltration upon combination treatment, without significant change in CD4$^+$, CD8$^+$ and programmed cell death protein 1 (PD1$^+$) cells. *Dark dashed lines* inside the violin plot indicate the median, *light dashed lines* indicate the interquartile range. *P* value determined by analysis of variance (ANOVA) with Tukey's post hoc test (*bottom*). (*F*) Representative images of histologic hematoxylin-eosin (HE) stains and immune histochemical analysis for CD3 expression of tissue sections of tumors from orthotopically transplanted mice. *Scale bars*, 50 μmol/L (*right*). CD3 quantification in 5 mice (n = 5 high-power fields each). *P* value determined by ANOVA with Tukey's post hoc test (*left*). (*G*) snRNAseq of tumors from orthotopically transplanted mice treated with vehicle, subasumstat, copanlisib, or the combination. Uniform Manifold Approximation and Projection (UMAP) colored according to cell types (*left*). Visualization of the cell density within each cohort (embedding density estimation). (*H*) UMAP colored according to T-cell phenotype (*left*). Visualization of the cell density within each condition (embedding density estimation). (*I*) Mean expression of *Xcl1* and *Il18r1* in T-cell cluster per pseudobulk expression. *P* values are based on pseudobulk differential expression genes. (*J*) Representative images of tissue sections of tumors from orthotopically transplanted mice upon treatment, labeled with 4′,6-diamidino-2-phenylindole (DAPI), Ki67, CD8, or chemokine ligand 5 (CCL5). *Scale bars*, 200 μm–20 μm (*top*). *P* value determined by ANOVA with Tukey's post hoc test (*bottom*). (*K*) UMAP colored according to macrophage phenotype (*left*). Visualization of the cell density within each condition, using embedding density estimation. (*L*) M2 score (*top*) M1 score (*bottom*) expression in the macrophage cluster upon no, monotreatment, or combination treatment. *Left*: UMAP plots for vehicle and combination treatment. *Center*: M2/M1 scores of all treatment groups. *Right*: Individual M1/M2 scores of the mean of each tumor. Box and whisker plot: The *boxes* indicate the 25th percentile (*bottom border*), median (*center line*), and 75th percentile (*top border*), the *whiskers* show the maximum and minimum ranges, and the *circles* indicate outliers. (*M*) Representative image of tissue sections of tumors from orthotopically transplanted mice upon treatment, labeled with DAPI and CD68, Scale bars, 200 μm–20 μm (top). *Bottom*: Quantification of CCL5 in CD68$^+$ cells. ROI, region of interest. *P* value determined by ANOVA with Tukey's post hoc test.

Despite the withdrawal of approval for the PI3Kα/δ-inhibitor copanlisib for relapsed indolent non-Hodgkin lymphoma after the Study of Copanlisib in Combination With Standard Immunochemotherapy in Relapsed Indolent Non-Hodgkin's Lymphoma (iNHL) (CHRONOS-4) phase 3 trial,[53] copanlisib demonstrated some clinical activity in *PIK3CA*-mutated cancer in the National Cancer Institute Molecular Analysis for Therapy Choice (NCI-'MATCH) Eastern Cooperative Oncology Group–American College of Radiology Imaging Network trial with a manageable toxicity profile,[54] pointing to the clinical potential of PI3Kα/δ inhibitors when applied as a principle.

PI3Kα/δi-SUMOi combination therapy enhanced recruitment of $CD3^+$ T cells in vivo in immunocompetent mice. After combination therapy, our snRNAseq analysis revealed robust expression of both CD4 and CD8 transcripts in tumor-infiltrating T cells, despite the absence of corresponding protein expression in some cases. This discrepancy suggests that the negative phenotype seen in cycIF and immune histochemical analysis may stem from transcriptionally active but protein-low or protein-suppressed cells, rather than representing a true expansion of double-negative T cells (DNTs). Although PI3Kα/δi-SUMOi–induced DNTs were associated with antitumor effects and changes in the TME in our in vivo model, other DNTs can promote cancer progression through immunosuppressive actions that support tumor growth and evade immune responses.[55] The anticancer properties of the DNTs could be induced by induction of immunogenic cell death,[56] and we show that RCD is activated in response to PI3Kα/δi-SUMOi combination therapy in in vitro studies. SUMO inhibition in vivo activated various immune cell subsets and reprogrammed the tumor immune microenvironment to induce an antitumor adaptive response.[17,57] We here found that PI3Kα/δi-SUMOi combination treatment was specifically associated with a molecular switch from protumorigenic M2-like macrophages to antitumorigenic antigen-presenting macrophages. Together our data thus indicate a multimodal reprograming of the TME toward a less tumor-permissive state upon PI3Kα/δi-SUMOi combination treatment. Furthermore, SUMOi generated an upregulation of major histocompatibility complex I expression.[37]

These established immune-modulatory effects of SUMO pathway inhibition might thus be amplified and beneficial when targeting PDAC with more effective rationale, molecularly targeted strategies such as combined PI3Kα/δ-SUMO inhibition. This mode of action of subasumstat also favors the combination with PI3Kis, given their broad impact on both intrinsic tumor survival pathways and the immune landscape.[8,58] PI3Kα/δi has been shown to modulate immune suppression within the TME, which may enhance the efficacy of immunotherapy-based approaches[59] that have been insufficiently effective in PDAC.[60] In this context, it is important that subasumstat generated a feed-forward loop by simultaneous activation of cytotoxic T cells and induction of the antigen-presenting machinery in PDAC and other tumor entities.[17,37]

Conclusion

In summary, we here reveal the mutual codependency between the SUMOylation machinery and the PI3K pathway that warrants further development toward clinical application. In addition to synthetic lethal effects induced on tumor cells, the PI3Kα/δi-SUMOi combination therapy induced affected immune cell subsets and resulted in the complex reprogramming of the TME to an antitumorigenic state in vivo. Our findings could serve as a novel path toward already available but heretofore unsuccessful immunotherapy strategies for PDAC.

Supplementary Material

Note: To access the supplementary material accompanying this article, visit the online version of *Gastroenterology* at www.gastrojournal.org, and at https://doi.org/10.1053/j.gastro.2025.08.018.

References

1. Buckley CW, O'Reilly EM. Next-generation therapies for pancreatic cancer. Expert Rev Gastroenterol Hepatol 2024;18:55–72.
2. Halbrook CJ, Lyssiotis CA, Pasca di Magliano M, et al. Pancreatic cancer: advances and challenges. Cell 2023;186:1729–1754.
3. Singhal A, Li BT, O'Reilly EM. Targeting KRAS in cancer. Nat Med 2024;30:969–983.
4. Dilly J, Hoffman MT, Abbassi L, et al. Mechanisms of resistance to oncogenic KRAS inhibition in pancreatic cancer. Cancer Discov 2024;14:2135–2161.
5. Schonhuber N, Seidler B, Schuck K, et al. A next-generation dual-recombinase system for time- and host-specific targeting of pancreatic cancer. Nat Med 2014;20:1340–1347.
6. Eser S, Reiff N, Messer M, et al. Selective requirement of PI3K/PDK1 signaling for Kras oncogene-driven pancreatic cell plasticity and cancer. Cancer Cell 2013;23:406–420.
7. Li H, Wen X, Ren Y, et al. Targeting PI3K family with small-molecule inhibitors in cancer therapy: current clinical status and future directions. Mol Cancer 2024;23:164.
8. Conway JR, Herrmann D, Evans TJ, et al. Combating pancreatic cancer with PI3K pathway inhibitors in the era of personalised medicine. Gut 2019;68:742–758.
9. He Y, Sun MM, Zhang GG, et al. Targeting PI3K/Akt signal transduction for cancer therapy. Signal Transduct Target Ther 2021;6:425.
10. Andre F, Ciruelos E, Rubovszky G, et al. Alpelisib for PIK3CA-mutated, hormone receptor-positive advanced breast cancer. N Engl J Med 2019;380:1929–1940.
11. Mateo J, Ganji G, Lemech C, et al. A first-time-in-human study of GSK2636771, a phosphoinositide 3 kinase beta-selective inhibitor, in patients with advanced solid tumors. Clin Cancer Res 2017;23:5981–5992.

12. Hong DS, Postow M, Chmielowski B, et al. Eganelisib, a first-in-class PI3Kgamma Inhibitor, in patients with advanced solid tumors: results of the phase 1/1b MARIO-1 Trial. Clin Cancer Res 2023; 29:2210–2219.
13. Borazanci E, Pishvaian MJ, Nemunaitis J, et al. A phase Ib study of single-agent idelalisib followed by idelalisib in combination with chemotherapy in patients with metastatic pancreatic ductal adenocarcinoma. Oncologist 2020;25:e1604–e1613.
14. Yue EW, Li YL, Douty B, et al. INCB050465 (parsaclisib), a novel next-generation inhibitor of phosphoinositide 3-kinase delta (PI3Kdelta). ACS Med Chem Lett 2019; 10:1554–1560.
15. Seeler JS, Dejean A. SUMO and the robustness of cancer. Nat Rev Cancer 2017;17:184–197.
16. Biederstadt A, Hassan Z, Schneeweis C, et al. SUMO pathway inhibition targets an aggressive pancreatic cancer subtype. Gut 2020;69:1472–1482.
17. Kumar S, Schoonderwoerd MJA, Kroonen JS, et al. Targeting pancreatic cancer by TAK-981: a SUMOylation inhibitor that activates the immune system and blocks cancer cell cycle progression in a preclinical model. Gut 2022;71:2266–2283.
18. Tapia Contreras C, Falke JD, et al. KRAS(G) (12C)-inhibitor-based combination therapies for pancreatic cancer: insights from drug screening. Mol Oncol 2025; 19:295–310.
19. Sealover NE, Theard PT, Hughes JM, et al. In situ modeling of acquired resistance to RTK/RAS-pathway-targeted therapies. iScience 2024;27:108711.
20. Wu DM, Zhang T, Liu YB, et al. The PAX6-ZEB2 axis promotes metastasis and cisplatin resistance in non-small cell lung cancer through PI3K/AKT signaling. Cell Death Dis 2019;10:349.
21. Rittler D, Baranyi M, Molnar E, et al. The antitumor effect of lipophilic bisphosphonate BPH1222 in melanoma models: the role of the PI3K/Akt pathway and the small G protein Rheb. Int J Mol Sci 2019;20:4917.
22. Chen Y, Wang T, Du J, et al. The critical role of PTEN/PI3K/AKT signaling pathway in shikonin-induced apoptosis and proliferation inhibition of chronic myeloid leukemia. Cell Physiol Biochem 2018;47:981–993.
23. Singh H, Xiu J, Kapner KS, et al. Clinical and genomic features of classical and basal transcriptional subtypes in pancreatic cancer. Clin Cancer Res 2024; 30:4932–4942.
24. Mueller S, Engleitner T, Maresch R, et al. Evolutionary routes and KRAS dosage define pancreatic cancer phenotypes. Nature 2018;554:62–68.
25. Zhou X, An J, Kurilov R, et al. Persister cell phenotypes contribute to poor patient outcomes after neoadjuvant chemotherapy in PDAC. Nat Cancer 2023;4:1362–1381.
26. Muzumdar MD, Chen PY, Dorans KJ, et al. Survival of pancreatic cancer cells lacking KRAS function. Nat Commun 2017;8:1090.
27. Milton CK, Self AJ, Clarke PA, et al. A genome-scale CRISPR screen identifies the ERBB and UBA2 signaling networks as key determinants of response to PI3K inhibition in pancreatic cancer. Mol Cancer Ther 2020; 19:1423–1435.
28. Kunz K, Piller T, Muller S. SUMO-specific proteases and isopeptidases of the SENP family at a glance. J Cell Sci 2018;131.
29. Langston SP, Grossman S, England D, et al. Discovery of TAK-981, a first-in-class inhibitor of SUMO-activating enzyme for the treatment of cancer. J Med Chem 2021; 64:2501–2520.
30. Folkes AJ, Ahmadi K, Alderton WK, et al. The identification of 2-(1H-indazol-4-yl)-6-(4-methanesulfonyl-piperazin-1-ylmethyl)-4-morpholin-4-yl-thieno[3,2-d] pyrimidine (GDC-0941) as a potent, selective, orally bioavailable inhibitor of class I PI3 kinase for the treatment of cancer. J Med Chem 2008;51:5522–5532.
31. Liu N, Rowley BR, Bull CO, et al. BAY 80-6946 is a highly selective intravenous PI3K inhibitor with potent p110alpha and p110delta activities in tumor cell lines and xenograft models. Mol Cancer Ther 2013; 12:2319–2330.
32. Matasar MJ, Capra M, Ozcan M, et al. Copanlisib plus rituximab versus placebo plus rituximab in patients with relapsed indolent non-Hodgkin lymphoma (CHRONOS-3): a double-blind, randomised, placebo-controlled, phase 3 trial. Lancet Oncol 2021; 22:678–689.
33. Morschhauser F, Machiels JP, Salles G, et al. On-target pharmacodynamic activity of the PI3K inhibitor copanlisib in paired biopsies from patients with malignant lymphoma and advanced solid tumors. Mol Cancer Ther 2020;19:468–478.
34. Yang Q, Modi P, Newcomb T, et al. Idelalisib: first-in-class PI3K delta inhibitor for the treatment of chronic lymphocytic leukemia, small lymphocytic leukemia, and follicular lymphoma. Clin Cancer Res 2015; 21:1537–1542.
35. Schild C, Wirth M, Reichert M, et al. PI3K signaling maintains c-myc expression to regulate transcription of E2F1 in pancreatic cancer cells. Mol Carcinog 2009; 48:1149–1158.
36. Schneeweis C, Hassan Z, Schick M, et al. The SUMO pathway in pancreatic cancer: insights and inhibition. Br J Cancer 2021;124:531–538.
37. Demel UM, Boger M, Yousefian S, et al. Activated SUMOylation restricts MHC class I antigen presentation to confer immune evasion in cancer. J Clin Invest 2022; 132:e152383.
38. Lightcap ES, Yu P, Grossman S, et al. A small-molecule SUMOylation inhibitor activates antitumor immune responses and potentiates immune therapies in preclinical models. Sci Transl Med 2021;13:eaba7791.
39. Rannikko JH, Hollmen M. Clinical landscape of macrophage-reprogramming cancer immunotherapies. Br J Cancer 2024;131:627–640.
40. Hu WT, Li M, Ma PJ, et al. A silence catalyst: CCL5-mediated intercellular communication in cancer. Arch Toxicol 2025;99:2699–2712.
41. Thibault B, Ramos-Delgado F, Pons-Tostivint E, et al. Pancreatic cancer intrinsic PI3Kalpha activity

accelerates metastasis and rewires macrophage component. EMBO Mol Med 2021;13:e13502.
42. Gupta S, Ramjaun AR, Haiko P, et al. Binding of ras to phosphoinositide 3-kinase p110alpha is required for ras-driven tumorigenesis in mice. Cell 2007;129:957–968.
43. Baer R, Cintas C, Dufresne M, et al. Pancreatic cell plasticity and cancer initiation induced by oncogenic Kras is completely dependent on wild-type PI 3-kinase p110alpha. Genes Dev 2014;28:2621–2635.
44. Wu CY, Carpenter ES, Takeuchi KK, et al. PI3K regulation of RAC1 is required for KRAS-induced pancreatic tumorigenesis in mice. Gastroenterology 2014; 147:1405–1416.e7.
45. Edling CE, Selvaggi F, Buus R, et al. Key role of phosphoinositide 3-kinase class IB in pancreatic cancer. Clin Cancer Res 2010;16:4928–4937.
46. Torres C, Mancinelli G, Cordoba-Chacon J, et al. p110gamma deficiency protects against pancreatic carcinogenesis yet predisposes to diet-induced hepatotoxicity. Proc Natl Acad Sci U S A 2019;116:14724–14733.
47. Kaneda MM, Cappello P, Nguyen AV, et al. Macrophage PI3Kgamma drives pancreatic ductal adenocarcinoma progression. Cancer Discov 2016;6:870–885.
48. Hobbs GA, Baker NMOL/L, Miermont AM, et al. Atypical KRAS(G12R) mutant is impaired in PI3K signaling and macropinocytosis in pancreatic cancer. Cancer Discov 2020;10:104–123.
49. Cintas C, Douche T, Dantes Z, et al. Phosphoproteomics identifies PI3K inhibitor-selective adaptive responses in pancreatic cancer cell therapy and resistance. Mol Cancer Ther 2021;20:2433–2445.
50. Psakhye I, Jentsch S. Protein group modification and synergy in the SUMO pathway as exemplified in DNA repair. Cell 2012;151:807–820.
51. Enserink JM. Sumo and the cellular stress response. Cell Div 2015;10:4.
52. Sheng Z, Zhu J, Deng YN, et al. SUMOylation modification-mediated cell death. Open Biol 2021;11: 210050.
53. Zinzani PL, Wang H, Feng J, et al. CHRONOS-4: phase 3 study of copanlisib plus rituximab-based immunochemotherapy in relapsed indolent B-cell lymphoma. Blood Adv 2024;8:4866–4876.
54. Damodaran S, Zhao F, Deming DA, et al. Phase II study of copanlisib in patients with tumors with PIK3CA mutations: results from the NCI-MATCH ECOG-ACRIN Trial (EAY131) Subprotocol Z1F. J Clin Oncol 2022; 40:1552–1561.
55. Velikkakam T, Gollob KJ, Dutra WO. Double-negative T cells: setting the stage for disease control or progression. Immunology 2022;165:371–385.
56. Ahmed A, Tait SWG. Targeting immunogenic cell death in cancer. Mol Oncol 2020;14:2994–3006.
57. Erdem S, Lee HJ, Shankara Narayanan JSN, et al. Inhibition of SUMOylation induces adaptive antitumor immunity against pancreatic cancer through multiple effects on the tumor microenviro nmol/Lent. Mol Cancer Ther 2024;23:1597–1612.
58. Sivaram N, McLaughlin PA, Han HV, et al. Tumor-intrinsic PIK3CA represses tumor immunogenecity in a model of pancreatic cancer. J Clin Invest 2019; 129:3264–3276.
59. Carnevalli LS, Sinclair C, Taylor MA, et al. PI3Kalpha/delta inhibition promotes anti-tumor immunity through direct enhancement of effector CD8(+) T-cell activity. J Immunother Cancer 2018;6:158.
60. Brahmer JR, Tykodi SS, Chow LQ, et al. Safety and activity of anti-PD-L1 antibody in patients with advanced cancer. N Engl J Med 2012;366:2455–2465.

Received February 19, 2025. Accepted August 12, 2025.

Correspondence
Address correspondence to: Günter Schneider, MD, Department of Surgery, University Medical Center Göttingen, Robert-Koch-Str. 40, 37075 Göttingen, Germany. e-mail: guenter.schneider@med.uni-goettingen.de; or Ulrich Keller, MD, Department of Hematology, Oncology and Cancer Immunology, Campus Benjamin Franklin, Charité - Universitätsmedizin Berlin, Hindenburgdamm 30, 12203 Berlin, Germany. e-mail: ulrich.keller@charite.de; or Matthias Wirth, PhD, Department of Surgery, University Medical Center Göttingen, Robert-Koch-Str. 40, 37075 Göttingen, Germany, and Department of Hematology, Oncology and Cancer Immunology, Campus Benjamin Franklin, Charité - Universitätsmedizin Berlin, Hindenburgdamm 30, 12203 Berlin, Germany. e-mail: matthias.wirth@med.uni-goettingen.de.

Acknowledgments
The authors thank Judith-Achler Galitzki, Konstandina Isaakidis, Gerhild Fiolka, and Jennifer Appelhans for their excellent technical assistance and express their gratitude to the Sartorius Corporate Research Department for the support of this research. Illustrations were created with BioRender.com. Part of results shown are based on data generated by The Cancer Genome Atlas Research Network (https://www.cancer.gov/tcga). The authors thank the fluorescence-activated cell sorter core facility of the University Medical Center Göttingen (DFG project number 63915960).

CRediT Authorship Contributions
Hazal Köse, MSc (Conceptualization: Supporting; Data curation: Equal; Formal analysis: Equal; Funding acquisition: Supporting; Investigation: Equal; Methodology: Lead; Validation: Lead; Visualization: Equal; Writing – original draft: Supporting)
Christian Schneeweis, PhD (Data curation: Equal; Investigation: Equal; Methodology: Supporting; Validation: Equal)
Philipp Putze, MSc (Formal analysis: Equal; Methodology: Equal)
Constanza Tapia Contreras, PhD (Data curation: Supporting; Formal analysis: Supporting; Investigation: Equal)
Laura Ferreiro, MSc (Data curation: Supporting; Formal analysis: Supporting; Investigation: Supporting; Validation: Supporting)
Leonie Witte, PhD (Data curation: Supporting; Formal analysis: Supporting; Investigation: Supporting; Validation: Supporting)
Ilaria Deidda, MSc (Data curation: Supporting; Formal analysis: Supporting; Investigation: Supporting; Validation: Supporting)
Frederik Herzberg, MD (Formal analysis: Supporting; Methodology: Supporting)
Sophie Ebert, MSc (Investigation: Supporting; Validation: Supporting)
Juraj Jakubik, PhD (Formal analysis: Supporting; Methodology: Supporting)
Leoni Moldaner, MSc (Formal analysis: Supporting; Methodology: Supporting)
Jovan Todorovic, MD (Formal analysis: Supporting; Methodology: Supporting)
Isabelle Träger, MD (Investigation: Supporting; Validation: Supporting)
Chuanbing Zang, PhD (Investigation: Supporting; Validation: Supporting)
Uta M. Demel, MD (Validation: Supporting), Elisabeth Hessmann, MD (Resources: Equal)
Marieluise Kirchner, PhD (Formal analysis: Supporting; Investigation: Supporting; Methodology: Equal; Resources: Equal)
Simone Rhein, PhD (Formal analysis: Equal; Methodology: Equal)
Jens Hoffmann, PhD (Resources: Equal)
Zuzana Tatarova, PhD (Formal analysis: Supporting; Methodology: Equal; Resources: Equal)
Michael Ghadimi, MD (Resources: Equal)
Dieter Saur, MD (Methodology: Supporting; Resources: Supporting)
Kai Kappert, MD (Investigation: Supporting; Methodology: Supporting; Resources: Supporting)
Philipp Mertins, PhD (Methodology: Equal; Resources: Supporting)
Günter Schneider, MD (Conceptualization: Equal; Funding acquisition: Equal; Resources: Equal; Supervision: Equal; Writing – original draft: Equal)
Ulrich Keller, MD (Conceptualization: Equal; Funding acquisition: Equal; Project administration: Equal; Supervision: Equal; Writing – original draft: Equal)

Matthias Wirth, PhD (Conceptualization: Equal; Data curation: Equal; Formal analysis: Equal; Funding acquisition: Equal; Investigation: Equal; Project administration: Equal; Resources: Supporting; Supervision: Equal; Visualization: Lead; Writing – original draft: Equal)

Conflicts of interest

These authors disclose the following: Ulrich Keller received reimbursement for advisory board function, speaker honorarium, and travel support from Takeda for content unrelated to this manuscript. Hazal Köse, Ulrich Keller, Günter Schneider, and Matthias Wirth have filed a patent application related to aspects of this work (application number EP25189303.8, pending). The remaining authors disclose no conflicts.

Funding

This work was supported by funding from Deutsche Forschungsgemeinschaft (WI 6148/1-1 project number 529255113 to Matthias Wirth, KE 222/10-1 project number 494535244, KE 222/11-1 project number 58460329, and German Research Foundation Excellence Strategy - EXC 3118/1 - project number 533770413 to Ulrich Keller, and CRU5002 to Günter Schneider and Elisabeth Hessmann), German Cancer Aid (70115444 to Matthias Wirth and 700111944, 70114724, and 70116097 to Ulrich Keller), Hector-Stiftung (M2408 to Matthias Wirth), Wilhelm-Sander-Stiftung (2017.048.2 to Ulrich Keller, Günter Schneider, and Matthias Wirth), SPARK-BIH (to Hazal Köse, Ulrich Keller, and Matthias Wirth), and Stiftung Charité (Ulrich Keller) and The German Cancer Consortium (Zuzana Tatarova).

Data Availability

All data generated in this study provided within the article and its supplementary data files are available via online repositories or upon request. RNA sequencing and single nuclei RNA sequencing data are deposited at European Nucleotide Archive, accession number ENA ID: PRJEB83901; proteomics data are available via PRIDE ID: PXD059116. Supplementary Table1 CRISPR beta scores. Supplementary Table 2 drug screening data. All other raw data are available upon request from the corresponding authors.